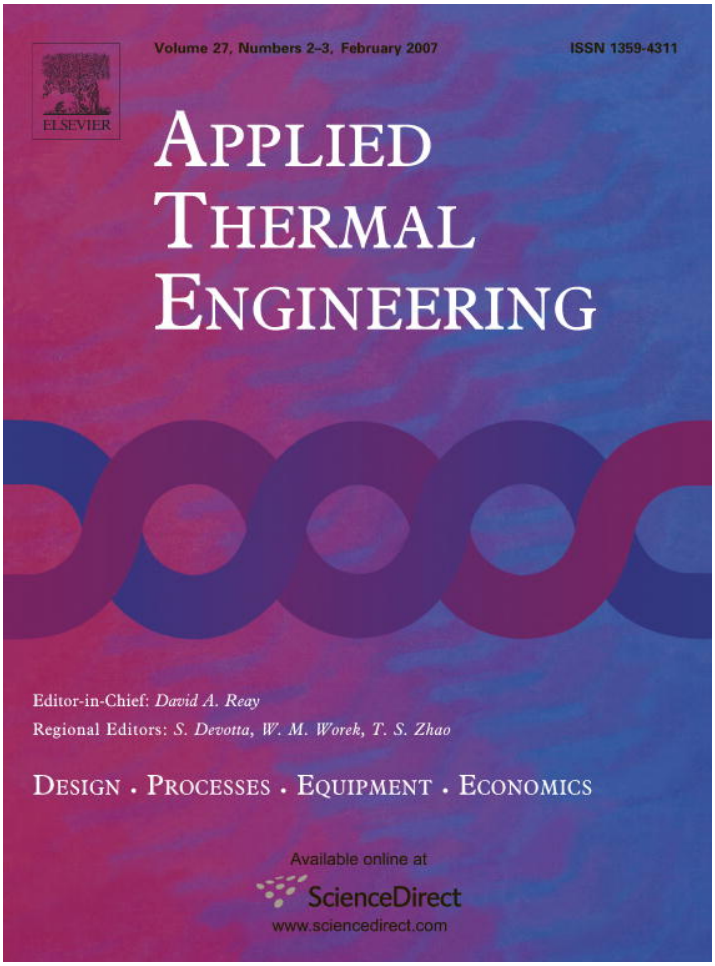

Available online at www.sciencedirect.com
ScienceDirect
Applied Thermal Engineering 27 (2007) 323–329
APPLIED THERMAL ENGINEERING
www.elsevier.com/locate/apthermeng

Monte Carlo simulations of gas flow and heat transfer in vacuum packaged MEMS devices

Hongwei Liu [a], Moran Wang [b,*], Jinku Wang [c], Guoyan Zhang [a], Huailin Liao [a], Ru Huang [a], Xing Zhang [a]

[a] *Institute of Microelectronics, Peking University, Beijing 100871, China*
[b] *Department of Mechanical Engineering, Johns Hopkins University, Baltimore, MD 21218, USA*
[c] *Department of Engineering Mechanics, Tsinghua University, Beijing 100084, China*

Received 14 October 2005; accepted 3 August 2006
Available online 29 September 2006

Abstract

The flow and heat transfer in vacuum packaged MEMS devices is numerically studied by using the direct simulation Monte Carlo method. The problem is simplified as an enclosure with a hot surface at the bottom. If the bottom is considered at a completely uniform high temperature, flow will be induced by the thermal stress difference from discontinuous temperature distribution effect. The heat transfer is weakened by the rarefied gas effect when compared with the continuum-based solution. If the bottom temperature is partly high and continuously decreases besides the hot part, the gas flow near the bottom surface will be remarkably enhanced due to the temperature gradients. As a result, the heat transfer on the hot chip surface is also enhanced. The current research can improve the understanding of gas flow and heat transfer in vacuum packaged MEMS devices.

Keywords: Monte Carlo simulation; Packaged MEMS device; Heat transfer; Gas flow; Chip cooling

1. Introduction

MEMS technique has been greatly developed since the late of 1980s, and was ever expected as emerging technologies with significant potential for future growth [1]. Micro systems based on MEMS are capable of sensing and controlling physical processes with length scales on the order of 1 μm, or even sub-micron [2–4]. Despite the growing number of realized applications of MEMS in scientific and engineering devices, there is only a minimum level of understanding of the fluid dynamics and heat transfer processes in fluidic MEMS. It was pointed that the technology was progressing at a rate that far exceeded that of our understanding of the unconventional physics involved in the operation as well as the manufacturing of those minute devices [5]. Performance of MEMS often defies predictions made using scaling laws developed for large systems. Therefore, there is a pressing need for reliable computational capabilities for understanding of the thermal and fluid dynamic processes in micro systems [6].

As well known, most MEMS devices have to be packaged before usage. To get a stable performance, a vacuum environment is generally needed when packaging. Although filling with a special gas is an alternative to reduce the cost remarkably, the vacuum package is a necessary requirement for some important applications [7,8]. The MEMS packages build up a closed system, including the chip, the gas (rarefied or not), and the package walls. The gas plays the role of transporting energies between the chip and the environment, so its flow and heat transfer characteristics are very important to the temperature-sensitive performance of the chip [9].

Rarefied or not, the gas in MEMS devices might have different behavior from the macroscopic gas due to the small characteristic length in MEMS. When the mean free

* Corresponding author.
E-mail address: moralwang@jhu.edu (M. Wang).

1359-4311/$ - see front matter © 2006 Elsevier Ltd. All rights reserved.
doi:10.1016/j.applthermaleng.2006.08.002

path of gas is at the same order of or even much larger than the system characteristic length, the continuum assumption will break down, and the traditional CFD techniques will therefore lead to large errors [10]. Such flows should be described using a molecular point of view [11,12]. The direct simulation Monte Carlo (DSMC) method, proposed by Bird [13,14] is the most successful numerical method for high Knudsen number gas flows. The DSMC method was validated by comparing with experimental data of rarefied gas flows in the last century [15,16]. In the past ten years, it has been used to predict the high Knudsen gas flow and heat transfer in microchannels [17–21]. Specially, the DSMC was recently extended to high Knudsen number non-ideal gas flow and heat transfer in micro- and nanochannels [22,23].

Though the rarefied gas flow behaviors in an enclosure have been studied much in the past years [24–28], the present paper focuses on the gas flow and heat transfer mechanism above a hot chip in micro square enclosures by using the DSMC method. The effects of wall temperature distributions on the gas flow and heat transfer will be concerned. The results are compared with continuum-based results. The factors influencing chip cooling in vacuum packaged MEMS devices are then summarized.

2. Numerical method

2.1. DSMC procedure

DSMC is a molecular-based statistical simulation method for rarefied gas flow introduced by Bird [13,14]. The method numerically solves the dynamic equations for gas flow using thousands of simulated molecules. Each simulated molecule represents a large number of real molecules. With the assumption of molecular chaos and a rarefied gas, only the binary collisions are considered, so the molecular motion and their collisions are uncoupled if the computational time step is smaller than the physical collision time. The interactions with boundaries and with other molecules conserve both momentum and energy. The macroscopic flow characteristics are obtained statistically by sampling the molecular properties in each cell.

At the beginning of the calculation, the simulated particles are uniformly distributed statistically in the cells. At each time step, all particles move according to their individual velocities, interact with the boundaries and then are indexed. In each cell, a certain number of collision pairs are selected using the no-time-counter (NTC) method and collisions are calculated. These steps are repeated to increase the sample size until the statistical errors are small enough. The DSMC method can simulate non-equilibrium and unsteady gas flow. A steady-state flow field is obtained with a sufficiently long simulation time. When the perfect gas assumption holds, the hard sphere model without intermolecular attractive potential is accurate enough for the collisions [18]. The present simulations used the variable hard sphere (VHS) model [14].

2.2. Discretization parameters

The cell size and time step for DSMC are very important parameters due to their direct effects on the results correctness. According to Bird [14], only when the computational time step is less than the mean collision time, could the molecular movements and collisions be decoupled. The cells are made small enough to restrict collisions to nearby particles but should contain a sufficient number of particles so that the method remains statistically accurate. Empirically, it has been found that cells should be no larger than a mean free path and contain at least twenty particles. Recently, the Green–Kubo formalism was used to quantitatively evaluate the dependence of the gas transport properties on the cell size [29,30] and the time step [31,32]. Recently, it has been numerically proved that the sub-cell size, instead of cell size, is limited no larger than the smallest mean free path in the domain [33]. In each case of this work, the cell (or sub-cell) size was always smaller than the local gas mean free path. The time step was then chosen as half of the smallest collision time in the channel. Each cell contained about twenty molecules, which ensures the accuracies of the simulations.

2.3. Statistical macroscopic quantities

Based on the kinetic theory [11,14], the macroscopic velocity is obtained by the statistic laws

$$\boldsymbol{u}_j = \frac{1}{N_j}\sum \boldsymbol{u}, \tag{1}$$

where **u** is macroscopic velocity vector, the subscript j represents the location index, i.e. the jth grid; and N_j is total number of simulated molecules in the jth grid during sample. For a diatomic gas, the Larsen–Borgnakke model with discrete rotational energy is used to model the energy exchange between the translational and internal modes. The vibrational energy is negligible. Therefore, the temperature can be obtained as

$$T = (3T_{\mathrm{tr}} + \zeta T_{\mathrm{rot}})/(3+\zeta), \tag{2}$$

where T_{tr} denotes the translational temperature, T_{rot} denotes the rotational temperature, and ζ is the number of internal degree of freedom. Both T_{tr} and T_{rot} are defined as

$$\frac{3}{2}kT_{\mathrm{tr}} = \overline{m\mathbf{v}^2} - \bar{m}\cdot\bar{\mathbf{v}}^2, \tag{3}$$

$$T_{\mathrm{rot}} = \frac{2}{k}(\overline{\varepsilon_{\mathrm{rot}}}/\zeta), \tag{4}$$

where k is the Boltzmann constant, **v** is the velocity vector of molecules, and $\varepsilon_{\mathrm{rot}}$ is the rotational energy of an individual molecule.

On the surface, the net heat transfer flux q is the sum of the translational and rotational energies of both the incident and the reflected molecules, i.e.

$$q = \frac{\left[\left(\sum_{i=1}^{n}\varepsilon_{\mathrm{tr}} + \sum_{i=1}^{n}\varepsilon_{\mathrm{rot}}\right)_{\mathrm{inc}} - \left(\sum_{i=1}^{n}\varepsilon_{\mathrm{tr}} + \sum_{i=1}^{n}\varepsilon_{\mathrm{rot}}\right)_{\mathrm{ref}}\right]N_0}{\Delta t \Delta x}, \tag{5}$$

where the subscripts "inc" and "ref" denote the incident and reflected molecular streams, respectively, n is the total number of simulated molecules that strike the wall during the sampling, N_0 is the number of gaseous molecules associated with a computational molecule, Δt is the time period of the sampling.

The codes developed based on the standard code of Bird's [14] have been validated for various micro geometries and different boundary conditions [18,21]. All calculated cases in this paper were performed on a Beowulf cluster, each CPU of which was 550 MHz. The sample size in each case was above 5×10^6, with which an acceptable accuracy could be obtained [34] though there are still obvious fluctuations in the results. The CPU time for each typical case is over 150 h.

3. Results and discussion

Here, we focus on the rarefied gas flow and heat transfer in a 2D micro square enclosure with a hot chip at the bottom by two cases. Firstly, assuming the whole bottom was a hot chip surface and the other sides were at an environment temperature, we simulate the flow and heat transfer in the enclosure by DSMC and compare with the continuum-based results. At the same time, the gravity effect on such flows and heat transfer are also checked. Secondly, we consider the hot chip is only at the central part of the bottom with damped temperature distributions beside both side to the environment temperature. The heat transfer mechanism is therefore discussed upon the simulation results and the data could be useful for design of MEMS devices.

3.1. Discontinuous temperature distribution effect

A simple model is shown in Fig. 1. The enclosure is made up of a uniform hot chip surface at the bottom and three walls. Each border length is L. The walls are isothermal at an environment temperature, T_{en}. The hot chip surface temperature is T_{c}. The joint points between the chip and the walls are therefore singular points with discontinuous temperature distributions. If the external force is ignored, according to the classical non-slip continuum theory, the flow should be absent and the heat transfer is pure heat conduction. When the rarefied gas effect is considered, the flow will be induced by the discontinuous temperature distribution [25–28]. Here, we focus on the effect factors influencing the gas flow and heat transfer above the chip surface. Consider a case where $L = 1$ mm, $T_{\mathrm{c}} = 600$ K, $T_{\mathrm{en}} = 300$ K, the initial nitrogen gas temperature is 300 K, and an initial Knudsen number is set 0.2. The gas is nitrogen gas, whose properties are listed in Table 1 [14].

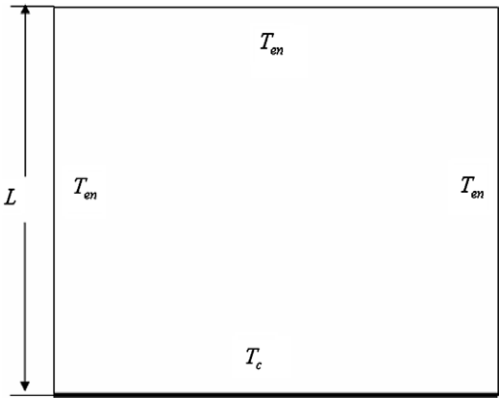

Fig. 1. Model of an enclosure with a uniform hot chip surface at bottom. T_{c} is the temperature of hot chip and T_{en} is the temperature of environment.

Table 1
Properties of nitrogen gas

m ($\times 10^{-26}$ kg)	ζ	d_{ref} ($\times 10^{-10}$ m)	T_{ref} (K)	ω	γ
4.65	2	4.17	273	0.74	1.4

where m is the gas molecular mass, ζ is the internal energy degrees of freedom, d_{ref} is the reference molecular diameter, T_{ref} is the reference temperature, ω is the viscosity–temperature index, and γ is the specific heat ratio.

The temperature contours and velocity vector field are shown in Fig. 2. Temperature jump and induced eddies are obvious from the figures. Similar results could also be found in previous work [28]. The temperature distribution deviates from that by pure heat conduction. Four remarkable eddies existed in the enclosure. The maximum value of velocity is less than but near 1 m/s, locating near both lower corners. The flow over the hot chip actually enhances the heat transfer process.

The heat flux along the hot chip surface at the bottom is plotted in Fig. 3, compared with the non-slip continuum-based solutions. The non-slip NS equations were solved by the commercial code Fluent 6 [35]. The gas properties and the boundary conditions in NS equations are selected as same as those in DSMC. Previous work has shown good agreements between continuum solutions and DSMC predictions at low Knudsen numbers [21,22]. As expected, the continuum solutions for the current case show no flow in the enclosure and pure heat conduction without external forces. However, it is surprising here to find that the heat flux resulted from DSMC is much lower than that from the continuum-based solution. To analyze the reason, the temperature distributions are compared in Fig. 4, which shows that the rarefied effect decreases greatly the temperature gradient near the surfaces. Go back to Fig. 2b, and we could find that each eddy can actually exchange energy with only one surface. As a result, although the gas flow velocity is not low, the heat transfer enhancement caused by flow cannot recuperate the weakening caused by the decreasing of temperature

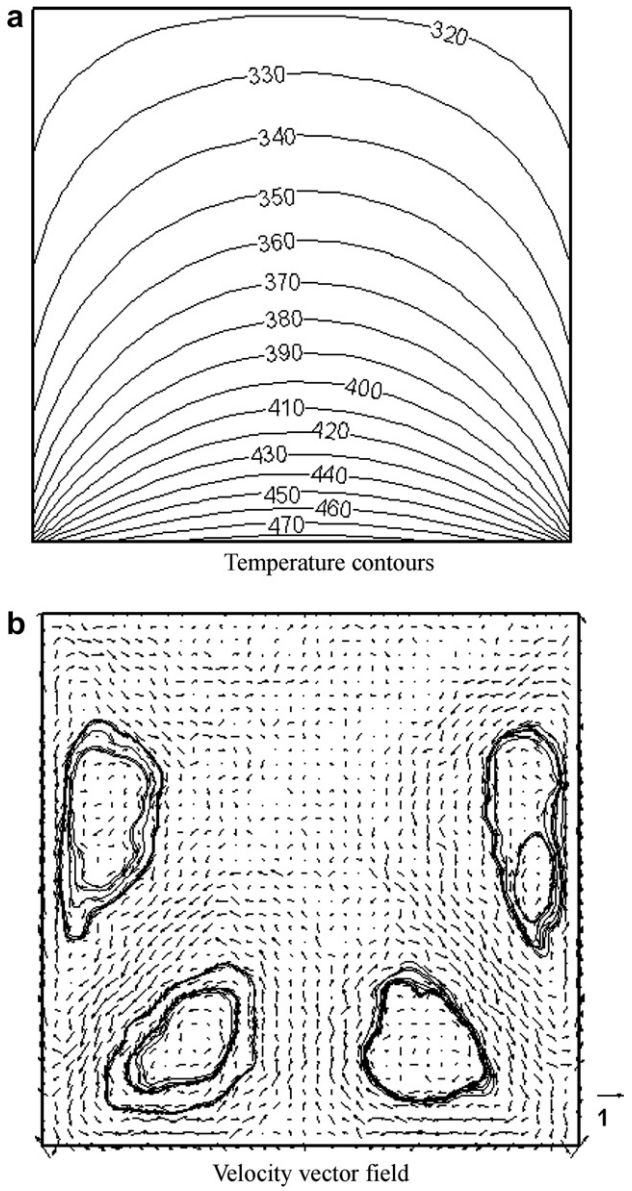

Fig. 2. Results for a uniform hot chip surface at the bottom, $Kn = 0.2$. The closed curves in (b) demonstrate streamlines: (a) temperature contours; (b) velocity vector field.

gradient near the surfaces. Therefore, for a vacuum packaged MEMS enclosure, heat transfer is actually weakened greatly by the rarefied gas effect, and heat transfer predictions by the classical NS solver will lead to significant overvaluations.

Many MEMS devices have special usages in aerospace systems. For such devices, the design, manufacture and test processes are mainly made on earth. Generally, it is thought that the gravity has little effect on rarefied gas flows and heat transfer. Here, we examine the gravity effects on the heat transfer in a packaged MEMS enclosure by numerical simulations. We model the gravity effect by adding an acceleration directly to each particle when moving. Fig. 6 compares the results between with and without gravity. The temperature distributions are almost the same.

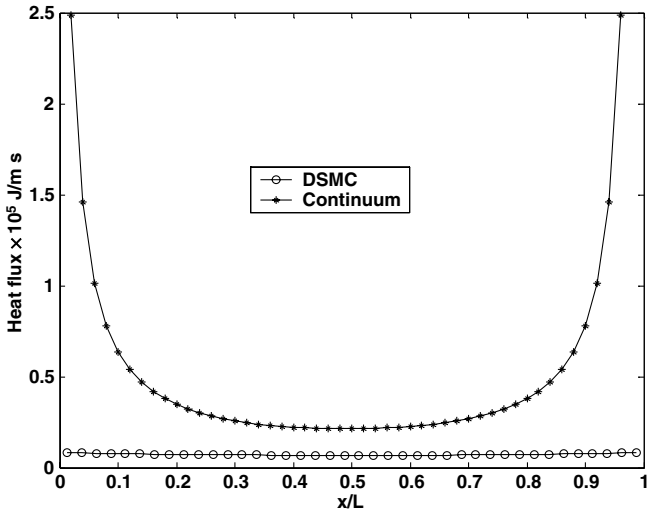

Fig. 3. Heat flux distributions along bottom surface.

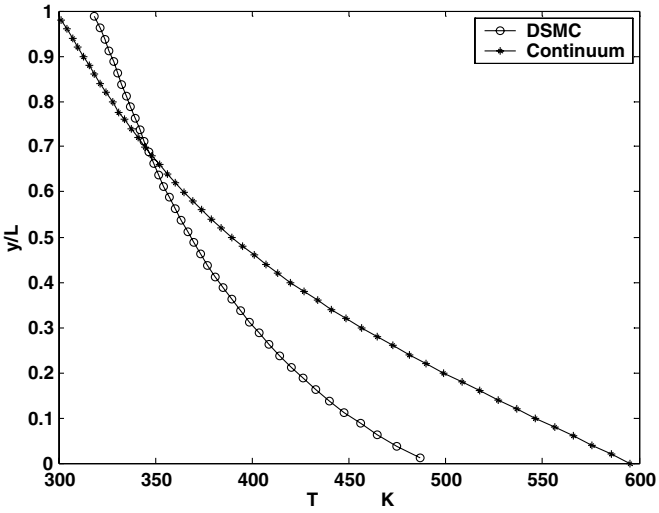

Fig. 4. Temperature distributions along the middle axis of symmetry.

The gravity enhances a little the heat transfer on the hot chip surface, but the effect was limited. The enhancement was less than 3% (see Fig. 5).

3.2. Temperature gradient effect

When a MEMS device is packaged, the main part of the device, the chip, is mostly located at the center of the bottom. There should be a distance left for operation convenience from the chip edge to the packaged wall. A simple scheme is shown in Fig. 6. When the chip is at a high temperature, the heat will conduct out, such as from A to C and from B to D. Thus continuous temperature gradients form from A to C and from B to D. Here consider a case very similar as that in Section 3.1. The chip temperature is $T_c = 600$ K, and the environment temperature is $T_{en} = 300$ K. The chip length $L_c = 2/5L$. The initial Knudsen number is 0.2.

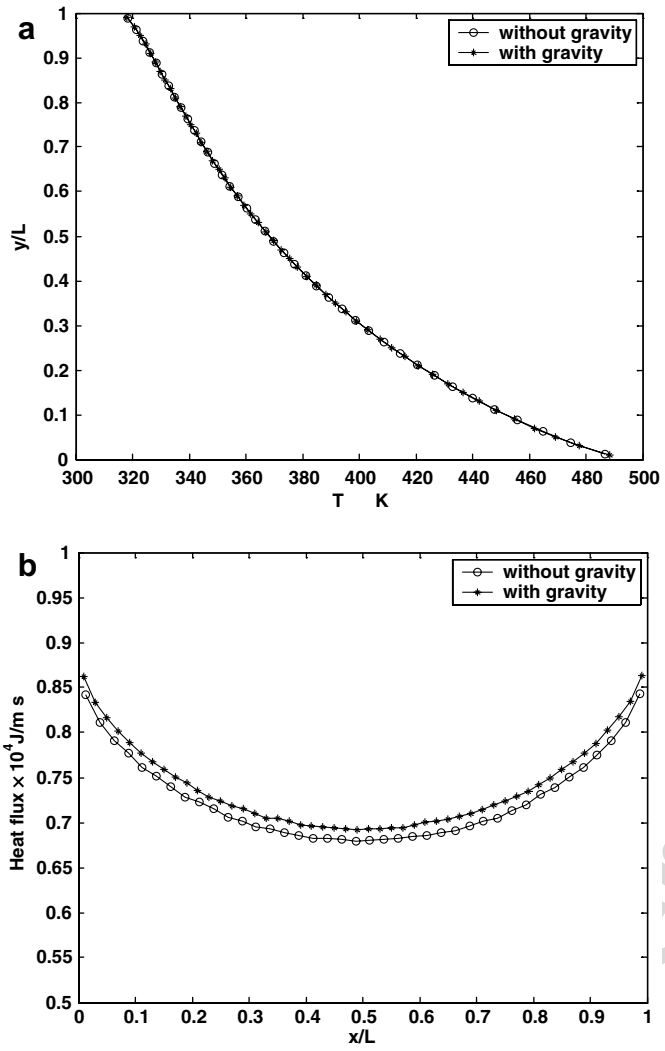

Fig. 5. Comparisons between with and without gravity: (a) temperature distributions along the middle axis of symmetry; (b) heat flux distributions along bottom surface.

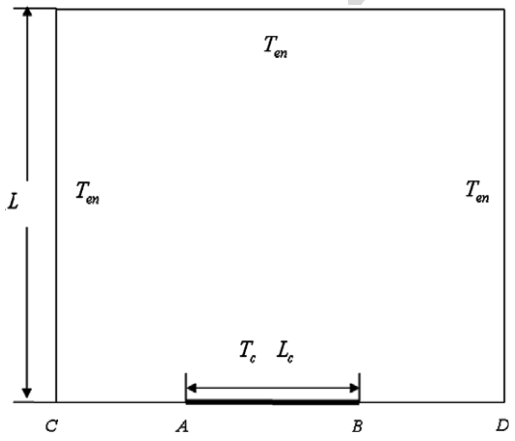

Fig. 6. Schematic for a partly hot chip at the bottom.

Fig. 7 shows the comparison of heat flux along the hot surface between the partly hot case and the completely hot case at the bottom. The heat flux with temperature gradient effect is much larger than that with a uniform temperature at the bottom. In rarefied gas, when temperature gradient exists on the surface, the gas will creep along the temperature gradient direction [26,27]. The velocity vector field is showed in Fig. 8. Two big eddies appear, each of which passes by two different temperature surfaces. Fig. 9 compares the x-velocity components of gas abut the bottom. The gas velocity caused by the creep effect is much larger than that by the thermal stress difference, which should be a main reason that enhances the heat transfer of the hot chip surface. These results show that if the enclosure bottom is not a completely uniform hot surface, the temperature gradient effect could not be ignored and might play a key role influencing the flow and heat transfer in the enclosure.

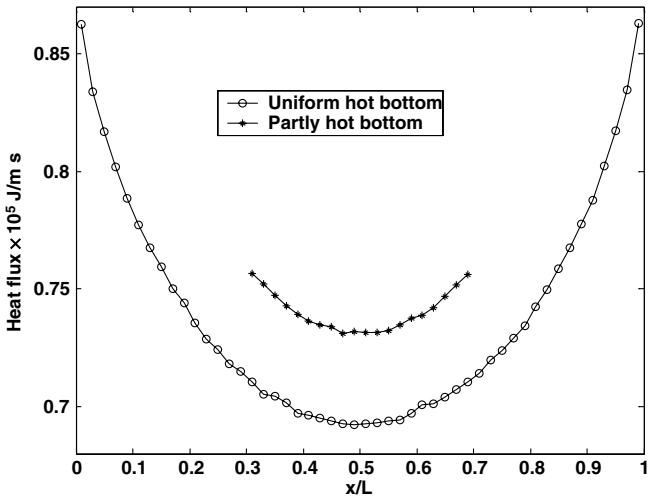

Fig. 7. Heat flux distribution along the hot (chip) surface.

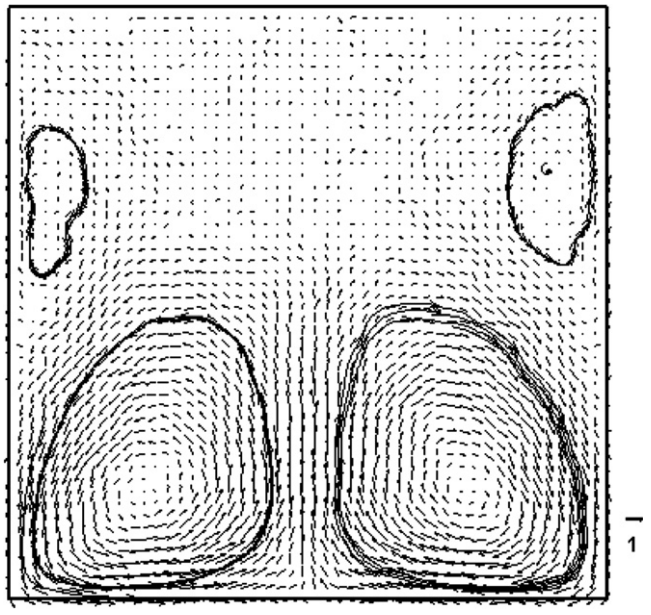

Fig. 8. Velocity field for temperature gradient effect at the bottom. The closed curves demonstrate streamlines.

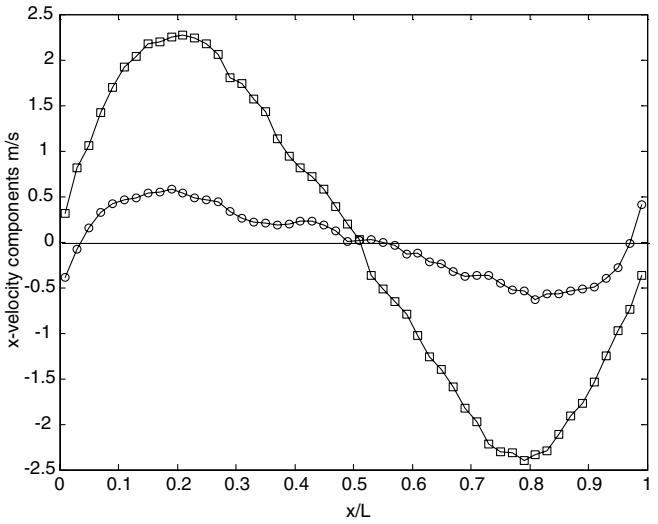

Fig. 9. The x-velocity components of gas abut the bottom. The circle (○) is the case for completely uniform hot bottom; the square (□) is for the partly hot with temperature gradient effect.

4. Conclusions

The flow and heat transfer in vacuum packaged MEMS devices is numerically investigated by the direct simulation Monte Carlo method. The results show that: when the bottom is a completely uniform hot chip, flow would be induced by the thermal stress difference of discontinuous temperature distribution effect. Compared with the non-slip continuum-based solution, the gas temperature gradient near the surfaces is much less when considering the rarefied gas effect. The heat transfer enhanced by the flow cannot recuperate the weakening by the decreasing of temperature gradient near the surfaces. Therefore, in packaged MEMS enclosure, the heat transfer is much weakened by the rarefied gas effect, and the classical NS predictions will lead to significant errors. For the low-pressure packaged MEMS device, the gravity has little effect on the flow and heat transfer.

If the bottom temperature is partly uniform at the center with temperature gradients besides the hot part, the gas flow near the bottom surface is remarkably enhanced due to the creep effect. As a result, the heat transfer on the hot chip surface is also enhanced comparing with the uniform temperature bottom case. The current research can provide significant insight for the understanding, design and optimization of packaged MEMS devices.

Acknowledgement

The present work was supported by the National Natural Science Foundation of China (Grant No. 59995550-2).

References

[1] S.E. Lyshevski, MEMS and NEMS: Systems, Devices, and Structures, CRC Press, 2002.
[2] H.A. Stone, A.D. Stroock, A. Ajdari, Engineering flows in small devices: microfluidics toward a lab-on-a-chip, Annu. Rev. Fluid Mech. 36 (2004) 381–411.
[3] Z.Y. Guo, Z.X. Li, Size effect on microscale single-phase flow and heat transfer, Int. J. Heat Mass Transfer 46 (2003) 149–159.
[4] T.S. Zhao, Q.C. Bi, Co-current air–water two-phase flow patterns in vertical triangular microchannels, Int. J. Multiphase Flow 27 (2001) 765–782.
[5] M. Gad-el-Hak, The fluid mechanics of microdevices-the freeman scholar lecture, J. Fluids Eng. 121 (1999) 5–33.
[6] M. Wang, Z.X. Li, Microscale thermal science and its applications in MEMS, Instrum. Tech. Sensor 7 (2002) 1–4.
[7] D.D.J.R. Evans, Advances in MEMS Packaging Advanced Packaging April, Published online, 2004 (http://ap.pennnet.com/Articles/Article_Display.cfm?Section=Articles&Subsection=Display&ARTICLE_ID=202290).
[8] H.A. Yang, M.C. Wu, W.L. Fang, Localized induction heating solder bonding for wafer level MEMS packaging, J. Micromech. Microeng. 15 (2005) 394–399.
[9] V.C. Hwang, Fabrication and characterization of a packaged MEMS gas flow sensor, in: 22nd Annual Microelectronic Engineering Conference, May, 2004, pp. 85–89.
[10] G.E. Karniadakis, A. Beskok, N.R. Aluru, Microflows and Nanoflows: Fundamentals and Simulation, Springer, 2005.
[11] E.H. Kennard, Kinetic Theory of Gases, McGraw-Hill, New York, 1938.
[12] C. Cercignani, Rarefied Gas Dynamics, From Basic Concepts to Actual Calculations, Cambridge University Press, 2000.
[13] G.A. Bird, Molecular Gas Dynamics, Clarendon Press, Oxford, 1976.
[14] G.A. Bird, Molecular Gas Dynamics and the Direct Simulation of Gas Flows, Clarendon, Oxford, 1994.
[15] G.A. Bird, Recent advances and current challenges for DSMC, Comput. Math. Appl. 35 (1998) 1–14.
[16] E.S. Oran, C.K. Oh, B.Z. Cybyk, Direct simulation monte carlo: recent advances and applications, Annu. Rev. Fluid Mech. 30 (1998) 403–441.
[17] W.W. Liou, Y. Fang, Heat transfer in microchannel devices using dsmc, J. MicroElectroMech. Syst. 10 (2001) 274–279.
[18] M. Wang, Z.X. Li, Similarity of ideal gas flow at different scales, Sci. China E 46 (2003) 661–670.
[19] C. Shen, J. Fan, C. Xie, Statistical simulation of rarefied gas flows in micro-channels, J. Comput. Phys. 189 (2003) 512–526.
[20] M. Wang, Z.X. Li, Simulations for gas flows in microgeometries using the direct simulation monte carlo method, Int. J. Heat Fluid Flow 25 (2004) 975–985.
[21] M. Wang, Z.X. Li, Numerical simulations on performance of MEMS-based nozzles at moderate or low temperatures, Microfluidics Nanofluidics 1 (2004) 62–70.
[22] M. Wang, Z.X. Li, Nonideal gas flow and heat transfer in micro- and nanochannels using the direct simulation Monte Carlo method, Phys. Rev. E. 68 (2003) 046704.
[23] M. Wang, Z.X. Li, Micro- and nanoscale non-ideal gas poiseuille flow in a consistent Boltzmann algorithm model, J. Micromech. Microeng. 14 (2004) 1057–1063.
[24] D.H. Papadopoulos, D.E. Rosner, Enclosure gas flows driven by non-isothermal walls, Phys. Fluids 7 (1995) 2535–2537.
[25] K. Aoki, S. Takata, H. Aikawa, F. Golse, A rarefied gas flow caused by a discontinuous wall temperature, Phys. Fluids 13 (2001) 2645–2661.
[26] Y. Sone, Flows induced by temperature fields in a rarefied gas and their ghost effect on the behavior of a gas in the continuum limit, Annu. Rev. Fluid Mech. 32 (2000) 779–811.
[27] Y. Sone, Kinetic Theory and Fluid Dynamics, Birkhauser, 2002.
[28] F. Yan, B. Karouk, discontinuous wall temperature distribution induced gas flow in an enclosure at high knudsen numbers, in: Proceedings of the International Heat Transfer Conference, Grenoble, France, August, 2002, pp. 513–518.
[29] F.J. Alexander, A.L. Garcia, B.J. Alder, Cell size dependence of transport coefficients in stochastic particle algorithm, Phys. Fluids 10 (1998) 1540–1542.

[30] F.J. Alexander, A.L. Garcia, B.J. Alder, Cell size dependence of transport coefficients in stochastic particle algorithm, Phys. Fluids 10 (1998) 1540, Erratum: Phys. Fluids 12 (2000) 731.
[31] A.L. Garica, W. Wagner, Time step truncation error in direct simulation Monte Carlo, Phys. Fluids 12 (2000) 2621–2633.
[32] N.G. Hadjiconstantinou, Analysis of discretization in the direct simulation Monte Carlo, Phys. Fluids 12 (2000) 2634–2638.
[33] M. Wang, Z.X. Li, Gas mixing in microchannels using the direct simulation Monte Carlo method, Int. J. Heat Mass Transfer. 49 (2006) 1696–1702.
[34] M.A. Rieffel, A method for estimating the computational requirements of DSMC simulations, J. Comput. Phys. 149 (1999) 95–133.
[35] Fluent 6.1.22 User's Guide, 2003.